

A Mixed Boundary Value Problem for a Finite Isotropic Wedge Under Antiplane Deformation

Bright Adinchezo Adimoha, James Nwawuike Nnadi, Bright Okore Osu and Franca Amaka Nwafor

Received: 19 July 2024/Accepted: 20 October 2024/Published: 26 October 2024

Abstract: This study investigates the behavior of singularities in a finite isotropic wedge subjected to antiplane deformation, focusing on how varying angles influence the strength of these singularities. Employing the finite Mellin transform technique, we derive solutions to the boundary value problems associated with the wedge configuration. The analysis reveals that as the angle α approaches critical values of $\frac{2\pi}{3}$, $\frac{3\pi}{4}$ and π , the strength of the singularity exhibits significant variations, specifically decreasing to $\frac{3}{4}$, $\frac{2}{3}$ and $\frac{1}{2}$, respectively. These findings underscore the critical relationship between the geometric configuration of the wedge and the resultant stress distribution around singularities. Furthermore, the implications of this research extend to practical engineering applications, highlighting the importance of understanding singularities in the design and analysis of structures under similar deformation conditions. Recommendations for further research include exploring additional geometric configurations, conducting experimental validations, and implementing numerical simulations to enhance the understanding of singular behavior in isotropic materials. This work contributes to the existing literature on boundary value problems and provides valuable insights for both theoretical and applied mechanics.

Keywords: Antiplane Deformation, Mixed Boundary, Mellin Transform, Stress Singularity, Stress Intensity Factor

Bright Adinchezo Adimoha

Department of Mathematics, Abia State University, Uturu, Abia State, Nigeria.

Email: adinohabright1980@gmail.com

James Nwawuike Nnadi

Department of Mathematics, Abia State University, Uturu, Abia State, Nigeria.

Email: profnnadij.n@gmail.com

Bright Okore Osu

Department of Mathematics, Abia State University, Uturu, Abia State, Nigeria.

Email:

Osu.bright@abiastateuniversity.edu.ng

Orcid id:0000-0003-2463-430X

Franca Amaka Nwafor

Department of Mathematics, Gregory University, Uturu, Nigeria

Email: amakanwaforfranca@gmail.com

1.0 Introduction

The finite Mellin transform is used to analyze the stress distribution throughout a finite isotropic wedge with radius a and wedge angle α , defined within the region described in cylindrical coordinates (r, θ, z) where $-\infty < z < \infty$, $-\alpha \leq \theta \leq \alpha$ and $0 \leq r \leq a$. The wedge is subjected to an anti-plane deformation condition by adjusting the radial boundaries. $\theta = \pm\alpha$, $0 \leq r \leq a$. The wedge is subjected to an anti-plane deformation condition by setting the radial boundaries to be stress-free and specifying displacement constraints. $W(a, \theta) = \gamma$, $0 \leq \theta \leq \alpha$. Let

α denote the angle on the upper part of the circular arc. $W(r, \theta)$ is the only non-vanishing component of the displacement, which is directed in the z-direction. The lower part of the circular arc, for which $-\alpha \leq \theta \leq 0$ is also stress-free.

Shahani(2005), Lin & Ma (2004), Shahani & Ghadiri (2009), Kargarnovin et al. (1997), and Chen et al. (2009) have examined problems involving isotropic finite wedges subjected to non-zero antiplane shear loads in the radial direction. The conditions applied to the entire circular arc of the wedges were either fixed or traction-free. Tranter(1948) used Mellin transform in finding the stress distribution in an infinite wedge.. Adimoha et al. (2024) analyzed the displacements in a finite isotropic wedge under antiplane shear deformation. In this study, we aim to understand the impact of this loading mode on the fracture response of a finite wedge, specifically in relation to the angles at which the stresses become

unbounded, the strength of geometric singularity, and the mode III crack tip stress intensity factor.

2.0 Basic Equations and Problem Solution

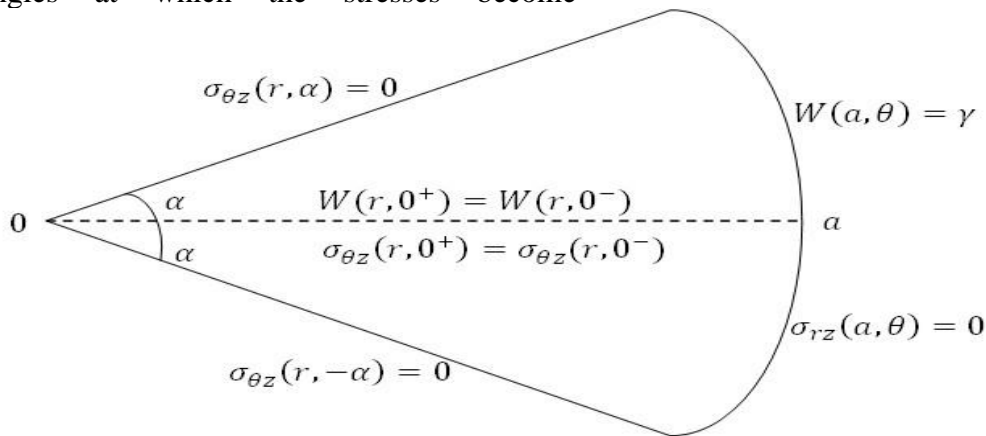
For this type of deformation, the shear stresses along the zzz-direction are the only remaining non-zero components in the constitutive equations, which can be expressed as follows:

$$\sigma_{rz}(r, \theta) = \mu \frac{\partial W(r, \theta)}{\partial r} \tag{1}$$

$$\sigma_{\theta z}(r, \theta) = \frac{\mu}{r} \frac{\partial W(r, \theta)}{\partial \theta} \tag{2}$$

where μ is the material shear modulus. In the absence of body forces, the equilibrium equation in terms of displacement leads to the Laplace equation, given by:

$$\left(\frac{\partial^2}{\partial r^2} + \frac{1}{r} \frac{\partial}{\partial r} + \frac{1}{r^2} \frac{\partial^2}{\partial \theta^2} \right) W(r, \theta) = 0, \quad 0 \leq r \leq a, \quad -\alpha \leq \theta \leq \alpha \tag{3}$$



Schematic Representation of the Finite Wedge

The boundary conditions are as follows:

$$\sigma_{\theta z}(r, \alpha) = 0, \quad 0 \leq r \leq a \tag{4}$$

$$\sigma_{\theta z}(r, -\alpha) = 0, \quad 0 \leq r \leq a \tag{5}$$

$$\sigma_{rz}(a, \theta) = 0, \quad -\alpha \leq \theta < 0 \tag{6}$$

$$W(a, \theta) = \gamma, \quad 0 < \theta < \alpha \tag{7}$$

The continuity conditions are as follows:

$$\bar{W}_{(1)}(s, \theta) = \int_0^a \left(\frac{a^{2s}}{r^{s+1}} - r^{s-1} \right) W(r, \theta) dr \tag{10}$$

The finite Mellin transform of the second kind is defined by:

$$\bar{W}_{(2)}(s, \theta) = \int_0^a \left(\frac{a^{2s}}{r^{s+1}} + r^{s-1} \right) W(r, \theta) dr \tag{11}$$

$$W(r, 0^+) = W(r, 0^-), \quad 0 \leq r \leq a \tag{8}$$

$$\sigma_{\theta z}(r, 0^+) = \sigma_{\theta z}(r, 0^-), \quad 0 \leq r \leq a \tag{9}$$

The solution of (3) can be obtained using the finite Mellin transform. The finite Mellin transform of the first kind is defined by:



where s is a complex transform parameter.

Once $\bar{W}_{(j)}(s, \theta)$ for $j = 1, 2$ are derived, the displacement $W(r, \theta)$ can be obtained using the inversion formula for these transforms as provided by Kargarnovin et al. (1997).

$$W(r, \theta) = \frac{(-1)^j}{2\pi i} \int_{c-i\infty}^{c+i\infty} \bar{W}_{(j)}(s, \theta) r^{-s} ds, \quad j = 1, 2 \tag{12}$$

Equation (10) applied to (3) produces

$$\left(\frac{d^2}{d\theta^2} + s^2\right) \bar{W}_{(1)}(s, \theta) + 2sa^2 W(a, \theta) = 0 \tag{13}$$

subject to the condition that:

$$\lim_{r \rightarrow 0} \left[(a^{2s} r^{-s} - r^s) r \frac{\partial W(r, \theta)}{\partial r} + s(a^{2s} r^{-s} + r^s) W(r, \theta) \right] = 0 \tag{14}$$

The finite Mellin transform of the second kind applied to (3) yields:

$$\left(\frac{d^2}{d\theta^2} + s^2\right) \bar{W}_{(2)}(s, \theta) + 2a^{s+1} \frac{\partial W(a, \theta)}{\partial r} = 0 \tag{15}$$

Provided that

$$\lim_{r \rightarrow 0} \left[(a^{2s} r^{-s} + r^s) r \frac{\partial W(r, \theta)}{\partial r} + s(a^{2s} r^{-s}) W(r, \theta) \right] = 0 \tag{16}$$

The range of values for s in the inversion formula (12) represents the regularity strip of $\bar{W}_{(j)}(s, \theta)$. This range is derived from the conditions (14) and (16). The asymptotic behavior of the stresses are

$$\sigma_{rz}(r, \theta) = \sigma_{\theta z}(r, \theta) = O(r^{-\lambda}), \quad 0 < \lambda < 1 \text{ as } r \rightarrow 0 \tag{17}$$

Hence

$$W(r, \theta) = O(r^{1-\lambda}) \text{ as } r \rightarrow 0 \tag{18}$$

The boundary data determine the type of finite Mellin transform to use. For this problem, the finite Mellin transform of the first kind is applied to equation (3) to obtain equation (13) with the boundary datum given in equation (7). The result is as follows:

$$\left(\frac{d^2}{d\theta^2} + s^2\right) \bar{W}_{(1)}(s, \theta) = -2sa^s \gamma, \quad 0 < \theta \leq \alpha \tag{19}$$

which is a non-homogeneous second-order ordinary differential equation. The solution of equation (19) can be expressed in the following form:

$$\bar{W}_{(1)}(s, \theta) = A_1(s) \sin \theta s + A_2(s) \cos \theta s - 2 \frac{a^s}{s} \gamma, \quad 0 < \theta \leq \alpha \tag{20}$$

The finite Mellin transform applied to equation (3), utilizing equations (15) and (6), leads to the following result:

$$\left(\frac{d^2}{d\theta^2} + s^2\right) \bar{W}_{(2)}(s, \theta) = 0, \quad -\alpha < \theta < 0 \tag{21}$$

whose solution can be expressed as:

$$\bar{W}_{(2)}(s, \theta) = B_1(s) \sin \theta s + B_2(s) \cos \theta s \tag{22}$$

The other boundary data are transformed using the transform of the second kind and equation (2) to obtain

$$\sigma_{\theta z}(r, \alpha) = \frac{\mu}{r} \frac{\partial W(r, \alpha)}{\partial \theta} = 0, \text{ for } \theta = \alpha, 0 \leq r \leq a$$

Consequently, $\frac{\partial \bar{W}(s, \alpha)}{\partial \theta} = 0$ at $\theta = \alpha$ when $0 < \theta \leq \alpha$ and $\sigma_{\theta z}(r, -\alpha) = \frac{\mu}{r} \frac{\partial W(r, -\alpha)}{\partial \theta}$, $\theta = -\alpha, -\alpha \leq \theta < 0, 0 \leq r \leq a$, which leads to

$$\frac{\partial \bar{W}(s, -\alpha)}{\partial \theta} = 0 \text{ at } \theta = -\alpha \text{ when } -\alpha \leq \theta < 0$$

Therefore, we seek $\bar{W}(s, \theta)$ that satisfies the boundary value problems (19) and (21) together with the conditions



$$\frac{d\bar{W}(s,\alpha)}{d\theta} = 0, \quad 0 < \theta \leq \alpha \tag{23}$$

$$\frac{d\bar{W}(s,-\alpha)}{d\theta} = 0, \quad -\alpha \leq \theta < 0 \tag{24}$$

$$\bar{W}(s, 0^+) = \bar{W}(s, 0^-) \tag{25}$$

$$\frac{d\bar{W}(s,0^+)}{d\theta} = \frac{d\bar{W}(s,0^-)}{d\theta} \tag{26}$$

We assume solutions of the forms (20) and (22) repeated as

$$\bar{W}(s, \theta) = A_1(s)\sin\theta s + A_2(s)\cos\theta s - 2\frac{a^s}{s}\gamma, \quad 0 < \theta < \alpha \tag{20}$$

$$= B_1(s)\sin\theta s + B_2(s)\cos\theta s, \quad -\alpha < \theta < 0 \tag{22}$$

The coefficients $A_i(s), B_i(s), i = 1,2$ are determined by use of the given boundary conditions.

From (20) and (22) we get

$$\frac{d\bar{W}(s,\theta)}{d\theta} = sA_1(s)\cos\theta s - sA_2(s)\sin\theta s, \quad 0 \leq \theta \leq \alpha \tag{27}$$

$$= sB_1(s)\cos\theta s - sB_2(s)\sin\theta s, \quad -\alpha \leq \theta \leq 0 \tag{28}$$

Application of (23) and (24) to (27) and (28) give

$$A_1(s)\cos\alpha s - A_2(s)\sin\alpha s = 0 \tag{29}$$

$$B_1(s)\cos\alpha s + B_2(s)\sin\alpha s = 0 \tag{30}$$

From (29) and (30) we get

$$(A_1(s) + B_1(s))\cos\alpha s + (B_1(s) - A_1(s))\sin\alpha s = 0 \tag{31}$$

Substitution of the continuity conditions (25) and (26) into (20) and (22) and then into (27) and (28) produce

$$A_2(s) - 2\frac{a^s}{s}\gamma = B_2(s) \tag{32}$$

and

$$A_1(s) = B_1(s) \tag{33}$$

Hence (31), (32) and (33) yield $2A_1(s)\cos\alpha s = -2\frac{a^s}{s}\gamma\sin\alpha s$ that gives,

$$B_1(s) = A_1(s) = \frac{a^s\gamma\sin\alpha s}{s\cos\alpha s} \tag{34}$$

Using (29), (30) and (33) leads to

$$(A_2(s) + B_2(s))\sin\alpha s = 0$$

Thus

$$A_2(s) + B_2(s) = 0 \tag{35}$$

Considering (32) and (35) produces the simultaneous equations

$$A_2(s) - B_2(s) = 2\frac{a^s}{s}\gamma$$

$$A_2(s) + B_2(s) = 0$$

Hence

$$A_2(s) = \frac{a^s\gamma}{s}$$

and

$$B_2(s) = -\frac{a^s\gamma}{s}$$

Consequently, the transformed displacement is deduced as

$$\bar{W}(s, \theta) = -\frac{a^s\gamma}{s\cos\alpha s}\sin\alpha s\sin\theta s + \frac{a^s\gamma}{s}\cos\theta s - 2\frac{a^s\gamma}{s} \quad 0 < \theta \leq \alpha \tag{36}$$

$$= -\frac{a^s\gamma}{s\cos\alpha s}\sin\alpha s\sin\theta s - \frac{a^s\gamma}{s}\cos\theta s \quad -\alpha \leq \theta < 0 \tag{37}$$



The corresponding displacement fields are obtained by using the inverse Mellin transform (12) with $j = 1j$

For $0 < \theta \leq \alpha$, $0 \leq \alpha \leq \pi$ (36) is used to get

$$W(r, \theta) = \frac{\gamma}{2\pi i} \int_{c-i\infty}^{c+i\infty} \frac{\sin\theta s \sin\alpha s}{s \cos\alpha s} \left(\frac{r}{a}\right)^{-s} ds - \frac{\gamma}{2\pi i} \int_{c-i\infty}^{c+i\infty} \frac{(\cos\theta s - 2)}{s} \left(\frac{r}{a}\right)^{-s} ds \quad (38)$$

The terms in the integrand of (38) are meromorphic functions of s . Therefore, the integral can be evaluated using the residue method, guided by Jordan's lemma. To consider the wedge apex, the region where $r < a$ must be examined. By Jordan's lemma, we close the contour to include the negative real axis $Re < 0$ where Re denotes the real part only, in which case the integrand vanishes as $|s| \rightarrow \infty$.

Hence, the displacement field is

$$W(r, \theta) = \frac{2\gamma}{\pi} \sum_{n=0}^{\infty} \frac{\sin\theta(2n+1)\frac{\pi}{2\alpha}}{2n+1} \left(\frac{r}{a}\right)^{(2n+1)\frac{\pi}{2\alpha}}, \quad r < a \quad (39)$$

and

$$W(r, \alpha) = \frac{2\gamma}{\pi} \sum_{n=0}^{\infty} \frac{(-1)^n}{2n+1} \left(\frac{r}{a}\right)^{(2n+1)\frac{\pi}{2\alpha}}, \quad r < a \quad (40)$$

By the Weierstrass M-test, the displacement given in (39) is uniformly and absolutely convergent. We may take

$$:u_n(\theta) = \frac{1}{2n+1} \sin\theta(2n+1)\frac{\pi}{2\alpha} \left(\frac{r}{a}\right)^{(2n+1)\frac{\pi}{2\alpha}} \text{ and } m_n = \frac{1}{2n+1} \left(\frac{r}{a}\right)^{(2n+1)\frac{\pi}{2\alpha}}$$

Application of the ratio test shows that $\sum_{n=0}^{\infty} m_n$, $r < a$ is convergent.

For $-\alpha \leq \theta < 0$, $-\pi \leq \alpha < 0$ with (37) and $j = 1$ in (12), we get

$$W(r, \theta) = \frac{\gamma}{2\pi i} \int_{c-i\infty}^{c+i\infty} \frac{\sin\theta s \sin\alpha s}{s \cos\alpha s} \left(\frac{r}{a}\right)^{-s} ds + \frac{\gamma}{2\pi i} \int_{c-i\infty}^{c+i\infty} \frac{\cos\theta s}{s} \left(\frac{r}{a}\right)^{-s} ds$$

By applying residue theory and analogous analysis in the evaluation of (39), the solution corresponding to the second integral is discarded because it is a constant. The solution derived from the first integral is precisely the one presented in (39). Therefore, it follows that

$$:W(r, 0^+) = W(r, 0^-) = 0 \quad (41)$$

Hence the line of symmetry, $\theta = 0$ is not deformed and

$$W(r, -\alpha) = -\frac{2\gamma}{\pi} \sum_{n=0}^{\infty} \frac{(-1)^n}{2n+1} \left(\frac{r}{a}\right)^{(2n+1)\frac{\pi}{2\alpha}}, \quad r < a \quad (42)$$

The corresponding stresses are obtained from (1), (2) and (39), for $0 < \theta \leq \alpha$ and $-\alpha \leq \theta < 0$ as

$$\sigma_{\theta z}(r, \theta) = \frac{\mu\gamma}{\alpha} \sum_{n=0}^{\infty} \cos\theta(2n+1)\frac{\pi}{2\alpha} \left(\frac{r}{a}\right)^{(2n+1)\frac{\pi}{2\alpha}-1}, \quad r < a \quad (43)$$

hence

$$\sigma_{\theta z}(r, 0^+) = \sigma_{\theta z}(r, 0^-) = \frac{\mu\gamma}{\alpha} \sum_{n=0}^{\infty} \left(\frac{r}{a}\right)^{(2n+1)\frac{\pi}{2\alpha}-1}, \quad r < a \quad (44)$$

If $\frac{\pi}{2} < \alpha < \pi$, we have $\frac{\pi}{2\alpha} < 1$ and $\frac{\pi}{\alpha} > 1$. Then $\frac{\pi}{2\alpha} - 1 < 0$ applied to (44) indicates that

$\sigma_{\theta z}(r, 0^+) = \sigma_{\theta z}(r, 0^-)$ becomes unbounded as $r \rightarrow 0$. Also, from (39) and (1) we obtained,



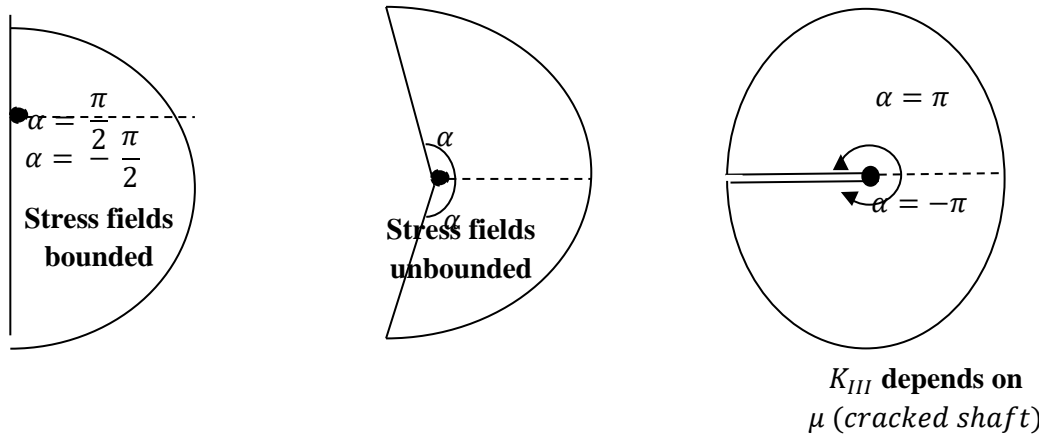
$$\sigma_{rz}(r, \theta) = \frac{\mu\gamma}{\alpha} \sum_{n=0}^{\infty} \sin\theta (2n + 1) \frac{\pi}{2\alpha} \left(\frac{r}{a}\right)^{(2n+1)\frac{\pi}{2\alpha}-1}, r < a \quad (45)$$

The fact that $0 < \alpha < \frac{\pi}{2}$ implies $\frac{\pi}{2\alpha} > 1$ and leads to $(2n + 1) \frac{\pi}{2\alpha} > 2n + 1$ or $(2n + 1) \frac{\pi}{2} - 1 > 2n$. Hence, by (39), the series solution for the displacement is bounded as $r \rightarrow 0, 0 < \alpha < \frac{\pi}{2}$.

From (43) and (45), the fields are bounded in a wedge with $0 < \alpha < \frac{\pi}{2}$. But, if $\frac{\pi}{2} < \alpha < \pi$ we have $\frac{\pi}{2\alpha} < 1$ and $(2n + 1) \frac{\pi}{2\alpha} < 2n + 1$ implies $(2n + 1) \frac{\pi}{2\alpha} - 1 < 2n$; the least value occurs when $n = 0$ for which $\frac{\pi}{2\alpha} - 1 < 0$. Therefore, the stress fields are unbounded as $r \rightarrow 0$, for $\frac{\pi}{2} < \alpha < \pi$. The asymptotic behaviours (17) yield the strength of geometry singularity as

$$\lambda = 1 - \frac{\pi}{2\alpha} \quad (46)$$

Consequently, when $\alpha = \frac{2\pi}{3}, \frac{3\pi}{4}$ and π the strength of singularity becomes $\frac{3}{4}, \frac{2}{3}$ and $\frac{1}{2}$ respectively.



The crack tip stress intensity factor can be derived using the formula provided by Shahani (2005).

$$K_{III} = \lim_{r \rightarrow 0} \sqrt{2\pi r} r^{\lambda_s} \sigma_{\theta z}(r, \alpha - \pi)$$

where λ_s is the order of stress singularity at the wedge apex. For this analysis, we refer to equation (43) to obtain the dominant term of the stress, which arises when $n = 0$ as follow:

$$\sigma_{\theta z}(r, \theta) = \frac{\mu\gamma}{\alpha} \cos\theta \frac{\pi}{2\alpha} \left(\frac{r}{a}\right)^{\frac{\pi}{2\alpha}-1}, r < a \quad (47)$$

when $\alpha = \pi$, the wedge resembles a circular shaft with an edge crack. In this scenario, the well-known square root singularity occurs at the crack tip. Consequently, the stress distribution near the crack tip can be characterized by a singularity of the form:

$$\sigma(r, \theta) \sim \frac{K}{r} \cdot f(\theta)$$

where K is the stress intensity factor, r is the distance from the crack tip, and $f(\theta)$ is a

function that describes the angular dependence of the stress field around the crack. This singularity is critical for understanding the local behavior of the material and the potential for crack propagation under applied loads.

Also, when $\alpha = \pi$, the wedge takes on the characteristics of a circular shaft with an edge crack. In this situation, the well-known square root singularity occurs at the crack tip. Therefore

$$\lambda_s = 1 - \frac{1}{2} = \frac{1}{2} \text{ and}$$

$$K_{III} = \sqrt{2\pi r} \frac{\mu\gamma}{a\alpha} \left(\frac{r}{a}\right)^{-\frac{1}{2}} = \sqrt{\frac{2\pi \mu\gamma}{a \alpha}}$$

The stress intensity factor depends on the material constants; however, it may also



exhibit a linear relationship with the apex angle α in certain cases, particularly when considering the shear modulus μ . Specifically, if the apex angle α varies linearly with the shear modulus, this relationship can influence the magnitude of the stress intensity factor, potentially modifying the stress distribution around the crack tip.

In general, the expression for the stress intensity factor K can be formulated as:

$$K = \sigma\sqrt{\pi a}$$

where σ is the applied stress and a is the crack length. If α and μ are related, the overall behavior of the stress intensity factor can be impacted by how these variables interact within the material's response to stress.

3.0 Conclusion

In this study, we investigated the behavior of singularities in a finite isotropic wedge under various angle conditions. Our findings indicate that as the angle α approaches specific critical values—namely $2\pi^3$, $3\pi^4$ and π —the strength of singularity exhibits notable variations. Specifically, we observed that at $\alpha = 2\pi^3$, the strength of the singularity is 34; at $\alpha = 3\pi^4$, it reduces to 23 and at $\alpha = \pi$, the singularity strength further diminishes to 12. These results underscore the critical role of the angle in influencing the stress distribution around singularities, thereby enhancing our understanding of deformation behaviors in isotropic materials.

Based on the outcomes of this study, we recommend that further research should be conducted to explore the effects of other geometric configurations and material properties on singularity strengths in various boundary value problems. Additionally, experimental studies should be carried out to validate the theoretical findings presented in this manuscript, particularly focusing on real-world applications where such singularities may occur. Future work could also include numerical simulations to analyze the behavior of singularities under dynamic loading

conditions, providing a more comprehensive understanding of the material response. The implications of these findings should be considered in engineering applications, particularly in the design of structures and materials subjected to similar conditions, to enhance their resilience and performance.

4.0 References

- Adimoha, B. A., Nnadi, J. N., Emenogu, G. N., & Osu, B. O. (2024). On the analysis of the displacements in a finite isotropic wedge under antiplane shear deformation. *International Journal of Computer Science and Mathematical Theory (IJCSMT)*, 10(6). (Accepted for publication). E-ISSN: 2545-5699, P-ISSN: 2695-1924. DOI: 10.56201/IJCSMT.
- Chen, C. H., Wang, C. L., & Ke, C. C. (2009). Analysis of composite finite wedges under antiplane shear. *International Journal of Mechanical Sciences*, 51, pp. 583-597.
- Kargarnovin, M. H., Shahani, A. R., & Fariborz, S. J. (1997). Analysis of an isotropic finite wedge under antiplane deformation. *International Journal of Solids and Structures*, 37, 1, pp. 113-128.
- Lin, J., & Ma, W. (2004). Theoretical full-field analysis of dissimilar isotropic composite annular wedges under antiplane deformations. *International Journal of Solids and Structures*, 41, pp. 6041-6080.
- Shahani, A. R. (2005). Some problems in the antiplane shear deformation of bi-material wedges. *International Journal of Solids and Structures*, 42, pp. 3093-3113.
- Shahani, A. R., & Ghadiri, M. (2009). Analysis of bonded finite wedges with an interfacial crack under antiplane shear loading. *Journal of Mechanical Engineering Sciences*, 223(Part C), 2213-2223. Proceedings of the Institute of Mechanical Engineering.
- Tranter, C. J. (1948). The use of Mellin transform in finding the stress distribution



in an infinite wedge. *Quarterly Journal of Mechanics and Applied Mathematics*, 1, 125-130.

Compliance with Ethical Standards

Declaration

Ethical Approval

Not Applicable

Competing interests

The authors declare that they have no known competing financial interests

Funding

The author declared no source of external funding

Availability of data and materials

Data would be made available on request.

Author's Contribution

Conceptualization, Formulation, Analysis and Supervision(JNN, BOO , BAA); Validation and Visualization(BAA , JNN, BOO and FAN); Writing the original draft, Review and Editing (BAA and BOO); Funding (FAN , BAA, BOO and JNN).

